



Origin of oxygen species in Titan's atmosphere

S. M. Hörst,¹ V. Vuitton,^{1,2} and R. V. Yelle¹

Received 3 March 2008; revised 9 May 2008; accepted 18 May 2008; published 7 October 2008.

[1] The detection of O^+ precipitating into Titan's atmosphere by the Cassini Plasma Spectrometer (CAPS) represents the discovery of a previously unknown source of oxygen in Titan's atmosphere. The photochemical model presented here shows that those oxygen ions are incorporated into CO and CO_2 . We show that the observed abundances of CO, CO_2 and H_2O can be simultaneously reproduced using an oxygen flux consistent with the CAPS observations and an OH flux consistent with predicted production from micrometeorite ablation. It is therefore unnecessary to assume that the observed CO abundance is the remnant of a larger primordial CO abundance or to invoke outgassing of CO from Titan's interior as a source of CO.

Citation: Hörst, S. M., V. Vuitton, and R. V. Yelle (2008), Origin of oxygen species in Titan's atmosphere, *J. Geophys. Res.*, 113, E10006, doi:10.1029/2008JE003135.

1. Introduction

[2] The Saturnian system is oxygen rich. Observations from Earth-based observatories and planetary missions have detected O^+ , O_2^+ , O, OH, and H_2O near Saturn [Esposito *et al.*, 2005; Waite *et al.*, 2005a, 2005b; Hartle *et al.*, 2006]. Icy ring particles were once thought to be the primary source of oxygen in the Saturnian system, but results from the Cassini mission indicate that unexpected geological vents on Enceladus are likely the dominant source [Dougherty *et al.*, 2006; Waite *et al.*, 2006; Hansen *et al.*, 2006; Horányi *et al.*, 2008]. Titan has long been known to have significant quantities of CO, CO_2 , and H_2O in its atmosphere [Samuelson *et al.*, 1983; Lutz *et al.*, 1983; Coustenis *et al.*, 1998], but their origin was uncertain. Here, we explore the possibility that the formation of these atmospheric species is connected to the oxygen sources in the greater Saturnian system. The origin of these species, particularly CO, has implications for the origin and evolution of Titan and the synthesis of complex molecules in its atmosphere.

[3] CO is a remarkably stable molecule, and its discovery in Titan's atmosphere [Lutz *et al.*, 1983] led to investigations into whether the observed abundance is a primordial remnant, is supplied to the atmosphere from the interior or surface, or is delivered to the atmosphere from an external source. The existence of remnant primordial CO would place useful constraints on models for the origin and evolution of Titan in the Saturnian nebula. Thermochemical calculations imply that the main nitrogen- and carbon-bearing species in the solar nebula were either N_2 and CO or NH_3 and CH_4 [Prinn and Fegley, 1981]. Thus the existence of an N_2 - CH_4 atmosphere on Titan is not well understood. Some hypothesized that the N_2 on Titan

evolved from gases trapped in clathrates that were incorporated into Titan as it accreted [Owen, 1982]. This hypothesis also implies that CO was the main carbon-bearing species at the time of accretion and Titan should have had a primordial abundance of CO larger than observed today. ^{40}Ar would also have been incorporated in large amounts, thus the low ^{40}Ar abundance in Titan's atmosphere [Niemann *et al.*, 2005; Waite *et al.*, 2005b] suggests that this hypothesis is probably not correct. Alternatively, recent works consider the idea that the CH_4 in Titan's atmosphere came from the solar nebula and was incorporated into the satellite as a clathrate [Mousis *et al.*, 2002]. These models also assume that NH_3 was delivered to Titan in a similar manner, but was subsequently converted to N_2 through photochemistry or shock chemistry [Atreya *et al.*, 1978; McKay *et al.*, 1988]. Recently, another hypothesis has been advanced by Atreya *et al.* [2006], who argue that CO should be outgassed from Titan's interior. The primordial CO abundance in Titan's atmosphere represents a significant constraint on such models and the thermochemical conditions in the solar nebula. Clearly, it is important to establish whether the CO on Titan is primordial, originates from the interior or surface, or whether it could be due solely to external sources.

[4] Early investigations into external sources of CO in Titan's atmosphere postulated that the CO could be produced through a chemical reaction scheme that began with an influx of H_2O into the upper atmosphere from micrometeorite ablation [Samuelson *et al.*, 1983; Yung *et al.*, 1984; Toubanc *et al.*, 1995; Lara *et al.*, 1996; English *et al.*, 1996]. Though this idea was attractive, given the known sources of H_2O and the success of the models, the hypothesis must now be viewed as incorrect. The primary reaction in the scheme $OH + CH_3$ produces H_2O [Wong *et al.*, 2002], not CO as previously assumed. When the proper chemistry is included, an influx of H_2O or OH produces no significant CO abundance. CO_2 can be produced by an H_2O influx only if CO is already present ($OH + CO \rightarrow CO_2 + H$). Because of their inability to reproduce the observed CO abundance, some recent works have suggested the persistence of

¹Lunar and Planetary Laboratory, University of Arizona, Tucson, Arizona, USA.

²Now at Laboratoire de Planétologie de Grenoble, CNRS, Université Joseph Fourier, Grenoble, France.

primordial CO in the atmosphere [Wilson and Atreya, 2004] or volcanic outgassing of CO from Titan's interior [Baines et al., 2006] to explain the current presence of CO in Titan's atmosphere. We show that CO can have a solely external origin but requires an influx of O^+ rather than H_2O or OH. The detection of a sufficient flux of O^+ precipitating into Titan's atmosphere by the Cassini Plasma Spectrometer (CAPS) [Hartle et al., 2006] is consistent with this hypothesis. However, an influx of H_2O or OH is still necessary to explain the observed abundances of H_2O and CO_2 .

[5] In this study we concentrate on relatively simple oxygen-bearing molecules and associated radicals. More complicated chemistry is certainly occurring, though at a much lower rate. The presence of active oxygen species in the upper atmosphere implies that some fraction of these will be incorporated into the large organic molecules present in Titan's atmosphere [Vuitton et al., 2007, 2008]. This is an exciting topic for future investigations. Here we try to establish the processes that lead to the observed abundances of CO, CO_2 , and H_2O . Section 2 reviews the observations of these molecules and previous models. Section 3 describes the model and chemical pathways, section 4 discusses the results, and section 5 summarizes our findings and presents some closing thoughts.

2. Previous Work

2.1. Summary of Observations

[6] The observed abundances of CO_2 , CO, and H_2O in Titan's atmosphere (summarized in Table 1) place vital constraints on photochemical models and must be well understood before any attempts at modeling are made. In particular, although CO has been measured numerous times at many different wavelengths, the observations are not all consistent and the explanation has been a source of much disagreement. Below we discuss the observations of CO_2 , CO, and H_2O and present our interpretation of the inconsistent CO measurements.

[7] CO_2 was the first oxygen-bearing molecule discovered in Titan's atmosphere. Samuelson et al. [1983] used Voyager 1 Infrared Interferometer Spectrometer (IRIS) observations of the ν_2 band of CO_2 at 667 cm^{-1} to infer a CO_2 mole fraction of $1.5^{+1.5}_{-0.8} \times 10^{-8}$. Further analysis of the Voyager 1 data found a stratospheric mole fraction of $1.4^{+0.3}_{-0.5} \times 10^{-8}$ that was constant from pole to pole within the uncertainties [Coustenis et al., 1989, 1991; Coustenis and Bezar, 1995]. The Voyager 1 findings were confirmed by Voyager 2 and the Infrared Space Observatory (ISO) [Letourneur and Coustenis, 1993; Coustenis et al., 2003]. The Cassini Composite Infrared Spectrometer (CIRS) is especially useful for measuring CO_2 because its spectral resolution is an order of magnitude higher than Voyager IRIS, greatly aiding in the separation of the signatures of CO_2 , C_6H_6 , and HC_3N all of which absorb near 670 cm^{-1} [de Kok et al., 2007; Coustenis et al., 2007]. Analysis of CIRS observations in this spectral region imply a mole fraction of $1.5^{+0.4}_{-0.4} \times 10^{-8}$ that appears constant with latitude and altitude [Flasar et al., 2005; de Kok et al., 2007; Coustenis et al., 2007].

[8] The discovery of CO_2 in Titan's atmosphere by Voyager 1 led Lutz et al. [1983] to search for CO using the Mayall Telescope at the Kitt Peak Observatory. They

used the 3-0 rotation-vibration band of CO at $1.6\text{ }\mu\text{m}$ to calculate an abundance of 6.0×10^{-5} in Titan's troposphere. The CO 1-0 rotation-vibration band at $4.8\text{ }\mu\text{m}$ has also been used to measure the tropospheric abundance of CO; Noll et al. [1996] inferred a lower tropospheric CO abundance of $1.0^{+1.0}_{-0.5} \times 10^{-5}$, while Lellouch et al. [2003] derived a tropospheric CO abundance of $3.2^{+1.0}_{-1.0} \times 10^{-5}$.

[9] Muhleman et al. [1984] obtained the first stratospheric CO measurement from microwave observations made with the Owen's Valley Radio Observatory (OVRO). They observed the CO 1-0 rotational line and found a best fit stratospheric mole fraction of 6.0×10^{-5} assuming abundance is constant with altitude. Marten et al. [1988] observed the same line from Institut de Radioastronomie Millimétrique (IRAM) and derived a CO mole fraction of 2×10^{-6} , which is significantly smaller than the tropospheric value. This resulted in the idea that the CO mole fraction might decrease with altitude. This assertion contradicts photochemical models that all predict a uniform CO profile because of its long chemical lifetime ($\sim 1\text{ Ga}$) [Yung et al., 1984] and the fact that CO does not condense in Titan's atmosphere. However, [Hidayat et al., 1998] suggest that the [Marten et al., 1988] result is too low because the telescope parameters were not well understood at the time of their analysis. More recent OVRO observations of the CO 1-0 [Gurwell and Muhleman, 1995], 2-1, and 3-2 [Gurwell and Muhleman, 2000; Gurwell, 2004] rotational lines infer an abundance of approximately 5.0×10^{-5} in the stratosphere, in agreement with the previous OVRO observation [Muhleman et al., 1984]. Aside from the Marten et al. [1988] observation, the only microwave observations that do not find a CO mole fraction of approximately 5.0×10^{-5} are those of Hidayat et al. [1998], who observed the CO 1-0, 2-1, and 3-2 rotational lines. They found abundances of 2.9×10^{-5} at 60 km, 2.4×10^{-5} at 175 km, 4.8×10^{-6} at 350 km. They attributed the decrease in CO above 175 km in their profile to CO production in the lower atmosphere and CO destruction above 175 km. This prediction contradicts photochemical models and current understanding of Titan's atmosphere, and the authors did not suggest possible production or destruction mechanisms. López-Valverde et al. [2005] were unable to fit their measurements of nonthermal emissions from CO at $5\text{ }\mu\text{m}$ using the monotonically decreasing CO altitude profile inferred by Hidayat et al. [1998] and instead infer a 32 ppm CO mole fraction in the troposphere and a stratospheric CO abundance of 60 ppm.

[10] Cassini CIRS measured emission from CO rotational lines in the far-IR between 30 and 60 cm^{-1} . This spectral range had not previously been used to measure the CO abundance and provides an independent check on previous results [de Kok et al., 2007]. Assuming the CO mole fraction is constant with altitude and latitude, a mole fraction of $4.7^{+0.8}_{-0.8} \times 10^{-5}$ is inferred from the CIRS data [Flasar et al., 2005; de Kok et al., 2007]. The Visible and Infrared Mapping Spectrometer (VIMS), also aboard Cassini, inferred a similar stratospheric CO abundance ($3.2^{+1.5}_{-1.5} \times 10^{-5}$) from measurements of nightside thermal emissions from the CO 1-0 band around 4.6 and $4.7\text{ }\mu\text{m}$ [Baines et al., 2006].

[11] H_2O in Titan's atmosphere was detected by Coustenis et al. [1998] using ISO. They observed emission features of pure rotational H_2O lines at 227.8 cm^{-1} and 254 cm^{-1} .

Table 1. Summary of Measurements of Oxygen Species in Titan's Atmosphere

Altitude	CO (ppm)	Wavelength	Reference
Troposphere	60	1.57 μm	<i>Lutz et al.</i> [1983]
Troposphere	10 ⁺¹⁰ ₋₅	4.8 μm	<i>Noll et al.</i> [1996]
Troposphere	32 ⁺¹⁰ ₋₁₀	4.8 μm	<i>Lellouch et al.</i> [2003]
Stratosphere	60 ⁺⁴⁰ ₋₄₀	2.6 mm	<i>Muhleman et al.</i> [1984]
Stratosphere	2 ⁺² ₋₁	2.6 mm	<i>Marten et al.</i> [1988]
60 km	29 ⁺⁹ ₋₅	0.85–2.6 mm	<i>Hidayat et al.</i> [1998]
175 km	24 ⁺⁵ ₋₅	0.85–2.6 mm	<i>Hidayat et al.</i> [1998]
350 km	4.8 ^{+0.3} _{-0.15}	0.85–2.6 mm	<i>Hidayat et al.</i> [1998]
Stratosphere	50 ⁺¹⁰ ₋₁₀	2.6 mm	<i>Gurwell and Muhleman</i> [1995]
Stratosphere	52 ⁺⁶ ₋₆	1.3 mm	<i>Gurwell and Muhleman</i> [2000]
Stratosphere	51 ⁺⁴ ₋₄	0.9 mm	<i>Gurwell</i> [2004]
Stratosphere	60	4.8 μm	<i>López-Valverde et al.</i> [2005]
Stratosphere	45 ⁺¹⁵ ₋₁₅	150–500 μm	<i>Flasar et al.</i> [2005]
Stratosphere	32 ⁺¹³ ₋₁₅	4–5 μm	<i>Baines et al.</i> [2006]
Stratosphere	47 ⁺⁸ ₋₈	150–500 μm	<i>de Kok et al.</i> [2007]
Altitude	CO ₂ (ppb)	Wavelength	Reference
Stratosphere	15 ⁺¹⁵ ₋₈	15 μm	<i>Samuelson et al.</i> [1983]
Stratosphere	14 ⁺³ ₋₅	15 μm	<i>Coustenis et al.</i> [1989]
Stratosphere	11 ⁺⁵ ₋₅	15 μm	<i>Letourneur and Coustenis</i> [1993]
Stratosphere	20 ⁺² ₋₂	15 μm	<i>Coustenis et al.</i> [2003]
Stratosphere	16 ⁺² ₋₂	15 μm	<i>de Kok et al.</i> [2007]
Stratosphere	15 ⁺⁴ ₋₄	15 μm	<i>Coustenis et al.</i> [2007]
Altitude	H ₂ O (ppb)	Wavelength	Reference
400 km	8 ⁺⁶ ₋₄	39.4, 43.9 μm	<i>Coustenis et al.</i> [1998]
Stratosphere	≤0.9	53–91 μm	<i>de Kok et al.</i> [2007]

Assuming that the H₂O mole fraction is constant with height above the condensation level, they derive a mole fraction of $8^{+6}_{-4} \times 10^{-9}$ at 400 km [Coustenis et al., 1998]. CIRS looked for the rotational lines of H₂O between 110 and 190 cm⁻¹. They did not detect H₂O above the noise level and found a 3 sigma upper limit on the mole fraction of H₂O in Titan's stratosphere of 9×10^{-10} [de Kok et al., 2007].

[12] On the basis of these observations, we will use a CO₂ mole fraction of 1.5×10^{-8} and an H₂O mole fraction of 8×10^{-9} as targets for the stratosphere in our model. Although there has been much disagreement about the abundance of CO in Titan's atmosphere, the Cassini observations are consistent with all of the previous stratospheric measurements except those of Hidayat et al. [1998] and are fairly consistent with the more difficult tropospheric measurements. Taken as a whole, the CO observations possess no strong evidence for altitudinal or temporal variations and we will therefore use a constant CO mole fraction of 5×10^{-5} as a target for our model. Since the distributions of CO, CO₂ and H₂O in Titan's atmosphere appear to have no observable latitudinal variation, a one-dimensional model should be sufficient for modeling their abundances.

2.2. Summary of Previous Models

[13] Since the discovery of oxygen-bearing species in Titan's atmosphere, a variety of sources have been suggested. The formation of CO₂ from the reaction of OH and CO led Samuelson et al. [1983] to suggest that the source of CO₂ on Titan was a flux of H₂O from sputtering of icy satellite and ring material or micrometeorite ablation.

English et al. [1996] investigated micrometeorite ablation in Titan's atmosphere and found that peak ablation occurs around 750 km resulting in an integrated H₂O deposition rate of $3.1 \times 10^6 \text{ cm}^{-2} \text{ s}^{-1}$ referred to the tropopause [Lara et al., 1996]. From their detection of H₂O in the atmosphere of Saturn, Feuchtgruber et al. [1997] calculated a necessary external H₂O flux at Saturn of $3\text{--}50 \times 10^5 \text{ cm}^{-2} \text{ s}^{-1}$. These fluxes are similar to those required by previous photochemical models to reproduce the CO₂ abundance on Titan if the CO abundance is fixed to observations [Wilson and Atreya, 2004]. They are also similar to fluxes inferred from observations of H₂O in Titan's atmosphere [Samuelson et al., 1998; Coustenis et al., 1998].

[14] For many years, the reaction $\text{OH} + \text{CH}_3 \rightarrow \text{CO} + 2\text{H}_2$ was thought to be the source of CO in Titan's atmosphere. Thus, H₂O was the only oxygen source necessary for the formation of CO and CO₂. Accordingly, micrometeorite ablation has been invoked as a source of oxygen in Titan's atmosphere in many studies [Yung et al., 1984; Toubanc et al., 1995; Lara et al., 1996; English et al., 1996; Coustenis et al., 1998; Wilson and Atreya, 2004; de Kok et al., 2007]. However, laboratory results indicate that the reaction between CH₃ and OH is not the major pathway for the production of CO. Instead the reaction proceeds as $\text{OH} + \text{CH}_3 \rightarrow \text{H}_2\text{O} + \text{CH}_2$, essentially recycling the water that was destroyed by photolysis [Baulch et al., 1994; Pereira et al., 1997; Oser et al., 1992]. The importance of these results for Titan was first recognized by Wong et al. [2002]. It implies that H₂O from micrometeorite ablation cannot be the major source of CO in Titan's atmosphere. The correct products for $\text{OH} + \text{CH}_3$ have also been included in the comprehensive model of Wilson and Atreya [2004]. This fundamental difference between the models of Yung et al. [1984], Toubanc et al. [1995], and Lara et al. [1996] and the models of Wong et al. [2002] and Wilson and Atreya [2004] makes comparisons between the two sets of models irrelevant. Thus the discussion here will be limited to Wong et al. [2002] and Wilson and Atreya [2004]. However, all of the models are summarized in Table 2.

[15] The failure of the external H₂O hypothesis to explain the observed levels of CO led to searches for other sources. Wong et al. [2002] showed that an H₂O flux from micrometeorite ablation of $1.5 \times 10^6 \text{ cm}^{-2} \text{ s}^{-1}$ leads to a CO mole fraction of 1.8×10^{-6} , which is much smaller than the observed value. Then they assumed that there must be another source of CO and used a CO flux from the surface of $1.1 \times 10^6 \text{ cm}^{-2} \text{ s}^{-1}$. That model reproduced the observed CO mole fraction with a value of 5.2×10^{-6} . However, their model was designed to investigate the isotopic evolution of CO over Titan's history and they did not report their calculated values of CO₂ or H₂O so it is not possible to evaluate how well their model reproduced the observed oxygen-bearing species in Titan's atmosphere. The photochemical model of Wilson and Atreya [2004], was also unable produce enough CO to match observations using a larger H₂O influx from micrometeorite ablation of $5 \times 10^6 \text{ cm}^{-2} \text{ s}^{-1}$ referred to the surface. Their remedy was to fix the CO abundance to the observed value of 5×10^{-5} . They find that 54 percent of H₂O destroyed is recycled back to H₂O

Table 2. Summary of Previous Models

	Mole Fraction ^a			Boundary Conditions ^b		
	150 km		400 km	CO lower	CO upper	H ₂ O upper
	CO	CO ₂	H ₂ O			
<i>Ying et al.</i> [1984]	1.8×10^{-4}	8.0×10^{-9}	1.0×10^{-9}	$\phi = 0$	$\phi = 8.8 \times 10^4$	$\phi = -6.1 \times 10^5$
<i>Toublanc et al.</i> [1995]	2.0×10^{-6}	2.0×10^{-12}	3.0×10^{-9}	$\chi = 2.0 \times 10^{-6}$		$\phi = -1.5 \times 10^6$
<i>Lara et al.</i> [1996] (equilibrium)	1.0×10^{-5}					$\phi = -6.0 \times 10^6$
<i>Lara et al.</i> [1996] (alternative)	5.0×10^{-5}	1.5×10^{-8}	2.0×10^{-8}		$\phi = -1.6 \times 10^6$	$\phi = -6.2 \times 10^6$
<i>Wong et al.</i> [2002] (standard)	5.2×10^{-5}			$\phi = 1.1 \times 10^6$		$\phi = -1.5 \times 10^6$
<i>Wong et al.</i> [2002] (equilibrium)	1.8×10^{-6}					$\phi = -1.5 \times 10^6$
<i>Wilson and Atreya</i> [2004]	5.0×10^{-5}	2.0×10^{-8}	1.0×10^{-8}	$\chi = 5.0 \times 10^{-5}$		$\phi = -5.0 \times 10^6$

^aCO mole fractions in bold were fixed in the model.

^bAll fluxes are referred to the surface. Fluxes given in $\text{cm}^{-2} \text{s}^{-1}$.

and the OH radicals that are not recycled back to water almost always end up in CO₂. They were able to match the CO₂ observations by assuming an external source of water. Since they were unable to reproduce the CO observations, they conclude that the CO is likely primordial.

[16] The difficulties with the H₂O deposition models have led to numerous other suggestions for the origin of CO including surface and subsurface sources such as volcanic outgassing of CO trapped in ice from the solar nebula [*Lara et al.*, 1996; *Samuelson et al.*, 1983; *Baines et al.*, 2006], CO itself contained in micrometeorites [*Lara et al.*, 1996], CO supplied by cometary impacts [*Lellouch et al.*, 2003], a surface source such as an ocean [*Lara et al.*, 1996; *Dubouloz et al.*, 1989] or that the CO currently observed is the remanent of a much larger primordial atmospheric abundance [*Wilson and Atreya*, 2004; *Wong et al.*, 2002]. None of the models mentioned above considered the consequences of an external source of O or O⁺. We show below that the chemistry initiated by O or O⁺ (which is quickly converted to O) differs fundamentally from that initiated by H₂O or OH and does in fact lead to production of CO.

3. Model Calculations

3.1. Energetic O⁺ Deposition

[17] The Cassini Plasma Spectrometer (CAPS) detected oxygen ions precipitating into Titan's atmosphere (energies $\sim 1\text{keV}$) [*Hartle et al.*, 2006]. When oxygen ions enter Titan's atmosphere they lose energy both through electronic excitations and momentum transfer to the ambient molecules, primarily N₂. The altitude of deposition is determined by the stopping power, given by

$$\frac{dE}{dX} \approx n_b(S_e + S_n), \quad (1)$$

where S_e and S_n are the electronic and nuclear stopping cross sections and n_b is the density of molecules encountered [*Johnson*, 1990]. Experimentally determined stopping cross sections were not available for oxygen ions in nitrogen at the energies of interest. However, they can be estimated from empirical equations that match experimental measurements at higher energies (10 to 10^5 keV) [*Ziegler*, 1980, 1984]. The stopping power is used to calculate the column abundance required to stop the oxygen ions and the corresponding altitude is found using the model atmosphere discussed in section 3.3. For 1 keV oxygen ions, the

deposition altitude is approximately 1100 km. The deposition altitude as a function of oxygen ion energy is shown in Figure 1.

[18] The final charge and energy states of the deposited oxygen ions are important for determining subsequent participation in chemical reactions. Initially, the energetic beam is a mix of ions and neutrals; as the particles slow the neutral state becomes favored and we assume that the entire beam is converted to neutral oxygen. To determine the final energy states, we calculated emission cross sections for the excited states of neutral oxygen, O(¹S), O(³S), O(⁵S), and O(¹D) following the methods of *Edgar et al.* [1975] and *Ishimoto et al.* [1992]. We compared the calculated cross sections to the total charge transfer cross section for production of O from O⁺ + N₂ from *Moran and Wilcox* [1978]. For 1 keV oxygen ions in a mixed state (O(⁴S) (ground state) and O(²D) (excited state)), the charge transfer cross section is approximately 10^{-15}cm^2 . Of the excited oxygen states, O(¹D) has the largest emission cross section, approximately 10^{-17}cm^2 at 1 keV [*Moran and Wilcox*, 1978]. Since the emission cross sections are at least 2 orders of magnitude smaller than the total charge transfer cross section we assume that all of the oxygen ions end up as ground state oxygen (O(³P)) when they are deposited. *Lindsay et al.* [1998] showed that the charge transfer cross section for O⁺-N₂ is highly dependent on the initial energy state of the oxygen ions, particularly at lower energies where the cross section is an order of magnitude smaller for the ground states than for the excited states. This effect is not included here because there is no data on the cross sections for production of excited O⁺, but it could raise the deposition altitude. As discussed in section 3.3, this uncertainty is not likely to have any effect on the oxygen chemistry.

3.2. Chemistry

[19] We consider oxygen chemistry in a fixed background of N₂ and hydrocarbon species. *Lara et al.* [1996] have shown that the nitrogen chemistry has only a small effect on the hydrocarbon chemistry and our preliminary calculations indicate that this is true of the oxygen chemistry as well. Densities of the important hydrocarbon species are shown by *Vuitton et al.* [2008].

[20] The hydrocarbon network consists of 40 species, ~ 130 neutral-neutral reactions and ~ 40 photodissociations. It is based on the reaction list presented by *Vuitton et al.* [2006] and further extended to hydrocarbon species con-

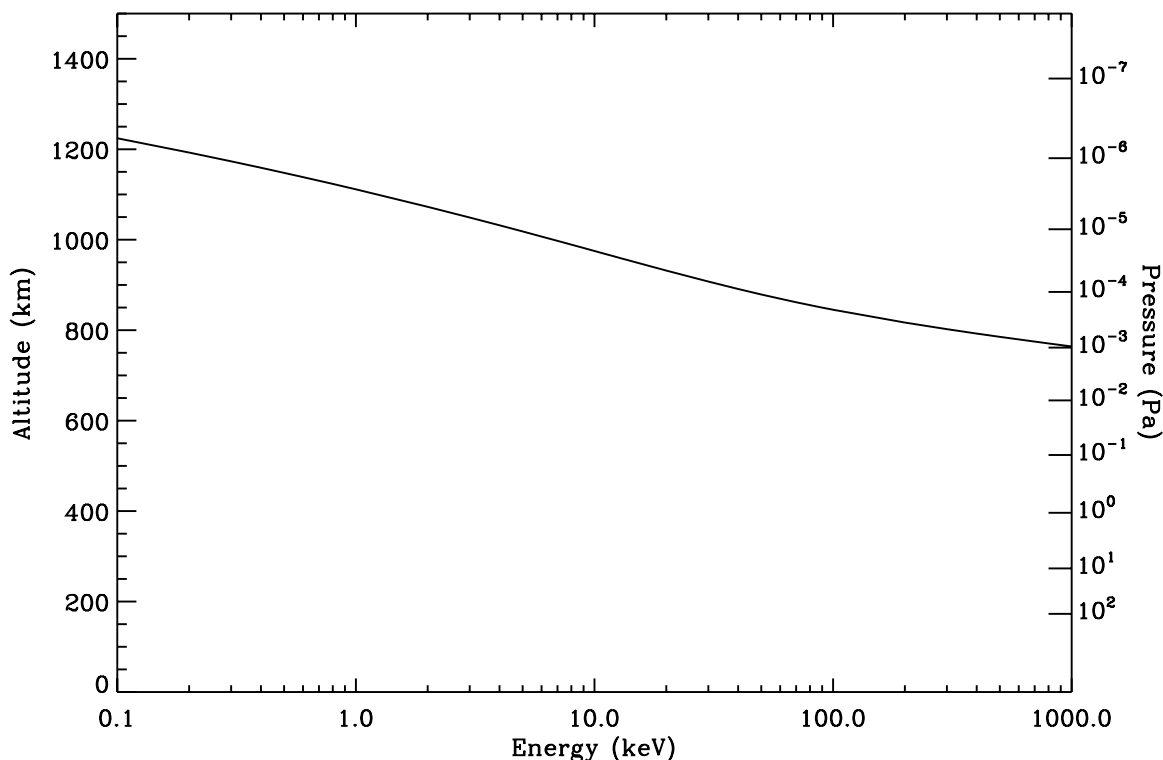


Figure 1. Deposition altitude of the oxygen ions as a function of their incident energy.

taining up to 6 carbon atoms [Vuitton *et al.*, 2008]. Heavier molecules produced are removed in the form of soot and are no longer involved in the chemistry. Ten oxygen-bearing species participating in 32 reactions have been added to the hydrocarbon network. Reviews and compilations of laboratory kinetic measurements provided the starting point for this reaction list [Atkinson *et al.*, 2006; Baulch *et al.*, 1994; Sander *et al.*, 2006].

[21] In the following, we discuss the main production and loss pathways for the 3 oxygen-bearing species that have been detected in Titan's atmosphere: H₂O, CO, and CO₂. We emphasize the improvements we made in our chemical scheme by comparison with previous photochemical models. The important chemical reactions involving oxygen species are listed in Table 3, and the photodissociation reactions for the oxygen species are listed in Table 4.

[22] Any H₂O deposited in the upper atmosphere is quickly transformed to OH because C₂H radicals efficiently abstract an H atom. However, H₂O is rapidly recycled by reaction of OH with CH₃ (k_{12a}). H₂O ultimately diffuses to the stratosphere where it is photodissociated to again produce OH radicals (J_{1a}). H₂O is recycled there by reaction of OH with CH₄ (k₁₃). It follows that a steady state between OH and H₂O is established throughout the atmosphere. If the input is OH instead of H₂O, OH is quickly transformed to H₂O by the same reactions and the OH/H₂O ratio and subsequent chemistry are very similar.

[23] Wong *et al.* [2002] were the first to recognize that the insertion of OH in CH₃ leads mostly to H₂O formation (k₁₂). This is drastically different from early photochemical models, which postulated that CO was the major product [Toublanc *et al.*, 1995; Lara *et al.*, 1996; Yung *et al.*, 1984]. As a consequence, the oxygen-bearing species distribution

was quite different in those models, since reaction k₁₂ was the major CO production process.

[24] CO can be readily produced by the insertion of incoming O(³P) with the radical CH₃ (k₇). If oxygen atoms are deposited in some excited state (O(¹D), O(¹S)), the excess energy is quickly released (k₁ – k₃) to produce O(³P) and the major product is again CO. If the source is in the form of O(¹D), a small fraction of the incoming oxygen (~5%) is transformed to OH by reactions with H₂ (k₄) and CH₄ (k_{5a}). As mentioned above, if the source of oxygen is in the form of OH, CO is only a minor product formed by secondary reactions of OH with CH₃ in the upper atmosphere (k_{12bc}) and C₂H₄ at lower altitude (k₁₅). The presence of CO₂ is explained exclusively by the reaction of OH with CO (k₁₆). This is the only loss mechanism for CO. CO₂ is mostly lost by condensation, while the importance of photolysis is heavily dependent on the value of the eddy coefficient in the lower atmosphere. Photolysis recycles CO₂ back to CO (J₃).

3.3. Description of Model Calculations

[25] In order to investigate the chemistry of oxygen-bearing species, we first construct a model for the distribution of temperature, density, and vertical mixing rate. The model covers the entire atmosphere, from the surface to 1500 km. We adopt a temperature-pressure profile derived by joining the Huygens Atmospheric Structure Instrument (HASI) and Huygens' Gas Chromatograph/Mass Spectrometer (GCMS) data [Fulchignoni *et al.*, 2005; Niemann *et al.*, 2005] at altitudes below 100 km, with results from the CIRS limb profiles [Vinatier *et al.*, 2007] from 100 to 500 km. At altitudes above 1000 km we use the empirical model of Müller-Wodarg *et al.* [2008], which is based on the Cassini

Table 3. Chemical Kinetics Reaction List for Oxygen-Bearing Species Along With Rate Coefficients, Temperature Range at Which the Rate Coefficients Were Measured/Calculated and References^a

R	Reaction	Rate Constant (k_{∞}/k_0)	T Range	Reference
k_1	$O(^1S) \rightarrow O(^1D)$	1.3×10^0	–	<i>Koyano et al.</i> [1975]
k_2	$O(^1D) \rightarrow O(^3P)$	6.7×10^{-3}	–	<i>Okabe</i> [1978]
k_3	$O(^1D) + N_2 \rightarrow O(^3P) + N_2$	$2.2 \times 10^{-11} \exp(+110/T)$	200–300	<i>Sander et al.</i> [2006]
k_4	$O(^1D) + H_2 \rightarrow OH + H$	1.1×10^{-10}	200–300	<i>Sander et al.</i> [2006]
k_{5a}	$O(^1D) + CH_4 \rightarrow OH + CH_3$	1.1×10^{-10}	200–300	<i>Sander et al.</i> [2006]
k_{5b}	$\rightarrow CH_3O + H$	3.0×10^{-11}	200–300	<i>Sander et al.</i> [2006]
k_{5c}	$\rightarrow HCHO + H_2$	7.5×10^{-12}	200–300	<i>Sander et al.</i> [2006]
k_{6a}	$O(^1D) + CO \rightarrow O(^3P) + CO$	$4.7 \times 10^{-11} \exp(+63/T)$	113–333	<i>Davidson et al.</i> [1978]
k_{6b}	$\rightarrow CO_2$	8.0×10^{-11b}	100–2100	<i>Tully</i> [1975]
		1.0×10^{-30b}	–	Estimated
k_{7a}	$O(^3P) + CH_3 \rightarrow HCHO + H$	6.9×10^{-11}	295	<i>Hack et al.</i> [2005]
k_{7b}	$\rightarrow CO + H_2 + H$	5.7×10^{-11}	295	<i>Hack et al.</i> [2005]
k_{8a}	$O(^3P) + HCO \rightarrow CO_2 + H$	5.0×10^{-11}	300–2500	<i>Baulch et al.</i> [1992]
k_{8b}	$\rightarrow CO + OH$	5.0×10^{-11}	300–2500	<i>Baulch et al.</i> [1992]
k_{9a}	$O(^3P) + CH_3CO \rightarrow CO_2 + CH_3$	2.6×10^{-10}	298–1500	<i>Baulch et al.</i> [1994]
k_{9b}	$\rightarrow CH_2CO^c + OH$	6.4×10^{-11}	298–1500	<i>Baulch et al.</i> [1994]
k_{10}	$OH + H_2 \rightarrow H_2O + H$	$7.7 \times 10^{-12} \exp(-2100/T)$	200–450	<i>Atkinson et al.</i> [2004]
k_{11}	$OH + ^3CH_2 \rightarrow HCHO + H$	3.0×10^{-11}	300–2500	<i>Tsang and Hampson</i> [1986]
k_{12a}	$OH + CH_3 \rightarrow H_2O + ^1CH_2$	$6.4 \times 10^{-8} T^{+5.8} \exp(+485/T)^d$	290–700	<i>Pereira et al.</i> [1997]
		$1.8 \times 10^{-8} T^{-0.91} \exp(-275/T)^d$	290–700	<i>Pereira et al.</i> [1997]
k_{12b}	$\rightarrow HCHO + H_2$	$1.1 \times 10^{-17} T^{+8.0} \exp(+1240/T)^d$	290–700	<i>Pereira et al.</i> [1997]
		$3.8 \times 10^{-14} T^{-0.12} \exp(+209/T)^d$	290–700	<i>Pereira et al.</i> [1997]
k_{12c}	$\rightarrow CH_3OH^c$	$7.2 \times 10^{-9} T^{-0.79b}$	290–700	<i>Pereira et al.</i> [1997]
		$1.1 \times 10^{-10} T^{-6.21} \exp(-671/T)^b$	290–700	<i>Pereira et al.</i> [1997]
k_{13}	$OH + CH_4 \rightarrow H_2O + CH_3$	$1.9 \times 10^{-12} \exp(-1690/T)$	200–300	<i>Atkinson et al.</i> [2006]
k_{14}	$OH + C_2H_2 \rightarrow CH_3CO$	$9.2 \times 10^{-18} T^{+2b}$	228–1400	<i>Sander et al.</i> [2006]
		5.5×10^{-30b}	228–1400	<i>Sander et al.</i> [2006]
k_{15}	$OH + C_2H_4 \rightarrow HOCH_2CH_2^c$	$1.1 \times 10^{-9} T^{-0.85b}$	96–296	<i>Sander et al.</i> [2006]
		$1.4 \times 10^{-17} T^{-4.5b}$	96–296	<i>Sander et al.</i> [2006]
k_{16a}	$OH + CO \rightarrow CO_2 + H$	$1.4 \times 10^{-13} (1 + [N_2])/4.2 \times 10^{19}$	200–300	<i>Atkinson et al.</i> [2006]
k_{16b}	$\rightarrow HOCO^c$	$1.8 \times 10^{-9} T^{-1.3b}$	200–300	<i>Sander et al.</i> [2006]
		$2.0 \times 10^{-36} T^{1.4b}$	200–300	<i>Sander et al.</i> [2006]
k_{17}	$HCO + H \rightarrow CO + H_2$	1.5×10^{-10}	300–2500	<i>Baulch et al.</i> [1992]
k_{18}	$HCO + CH_3 \rightarrow CO + CH_4$	2.0×10^{-10}	300–2500	<i>Tsang and Hampson</i> [1986]
k_{19}	$CH_3O + H \rightarrow HCHO + H_2$	3.0×10^{-11}	300–1000	<i>Baulch et al.</i> [1992]
k_{20}	$CH_3O + CH_3 \rightarrow HCHO + CH_4$	4.0×10^{-11}	300–2500	<i>Tsang and Hampson</i> [1986]
k_{21a}	$CH_3CO + CH_3 \rightarrow CO + C_6H_6$	5.4×10^{-11}	298	<i>Adachi et al.</i> [1981]
k_{21b}	$\rightarrow CH_2CO^c + CH_4$	1.0×10^{-11}	298	<i>Hassinen et al.</i> [1990]
k_{21c}	$\rightarrow CH_3COCH_3^c$	7.0×10^{-11b}	298	<i>Hassinen et al.</i> [1990]
		1.0×10^{-30b}	–	Estimated
k_{22}	$C_2H + H_2O \rightarrow OH + C_2H_2$	$2.1 \times 10^{-12} \exp(-200/T)$	295–451	<i>Vanlook and Peeters</i> [1995]

^aFor three-body reactions, low- and high-pressure rate coefficients are in italic and bold, respectively. Rate coefficients are in s^{-1} (unimolecular in bold), $cm^3 s^{-1}$ (bimolecular) or $cm^6 s^{-1}$ (termolecular in italic).

^bConventional Lindemann-Hinshelwood expression for three-body reactions: $k = (k_0 k_{\infty} [M]) / (k_0 [M] + k_{\infty})$, with k_0 and k_{∞} termolecular and bimolecular rate constants, respectively.

^cAssumed to ultimately produce CO, in particular CH_3OH photolyzes to form either CH_3O or $HCHO$ [*Harich et al.*, 1999; *Satyapal et al.*, 1989], which are quickly converted to CO.

^dModified Lindemann-Hinshelwood expression for three-body reactions: $k = (k'_0 k'_{\infty}) / (k'_0 [M] + k'_{\infty})$, with k'_0 and k'_{∞} bimolecular and unimolecular rate constants, respectively.

^eAssumed to ultimately produce CO_2 .

Ion and Neutral Mass Spectrometer (INMS) measurements. The region between 500 and 1000 km is modeled by interpolating between the CIRS and INMS results in the manner described by *Yelle et al.* [2008].

[26] The vertical mixing rate is a critical aspect of the oxygen chemistry on Titan but is impossible to predict from first principles. We model the vertical mixing with an empirical eddy diffusion coefficient, K , the general characteristics of which are well-established from previous inves-

tigations. The value in the lower stratosphere, from 50 to 100 km, must be very low in order to explain the large abundance of photochemically produced species in Titan's atmosphere. This assumption, first made by *Yung et al.* [1984], has been adopted in all Titan photochemical models. The essential requirement is that K must be small in the region just above where photochemical products condense so there is a barrier between the sources at high altitude and the sink at low altitude, resulting in a buildup of large

Table 4. Photodissociation Reactions for the Oxygen-Bearing Species Included in Our Model^a

No.	Reaction	Cross Section			Quantum Yield	
		Wavelength (nm)	Temp (K)	Reference	Wavelength (nm)	Reference
J_{1a}	$\text{H}_2\text{O} \rightarrow \text{OH} + \text{H}$	100–115	298	<i>Chan et al.</i> [1993a]	100–124	<i>Mordaunt et al.</i> [1994]
J_{1b}	$\rightarrow \text{O}(^1\text{D}) + \text{H}_2$	115–194	298	<i>Mota et al.</i> [2005]	124–140	<i>Stief et al.</i> [1975]
J_{1c}	$\rightarrow \text{O}(^3\text{P}) + \text{H} + \text{H}$				140–194	<i>Sander et al.</i> [2006]
J_2	$\text{CO} \rightarrow \text{C} + \text{O}(^3\text{P})$	6–60	298	<i>Chan et al.</i> [1993b]	6–100	<i>Okabe</i> [1978]
		60–100	295	<i>Cook et al.</i> [1965]		
J_{3a}	$\text{CO}_2 \rightarrow \text{CO}^{\text{a}} + \text{O}(^3\text{P})$	100–117	298	<i>Chan et al.</i> [1993c]	100–129	<i>Lawrence</i> [1972]
J_{3b}	$\rightarrow \text{CO} + \text{O}(^1\text{D})$	117–163	195	<i>Yoshino et al.</i> [1996]	129–300	<i>Okabe</i> [1978]
J_{3c}	$\rightarrow \text{CO} + \text{O}(^1\text{S})$	163–192	195	<i>Parkinson et al.</i> [2003]		
		192–300	298	<i>Shemansky</i> [1972]		
J_4	$\text{HCO} \rightarrow \text{CO} + \text{H}$	613–616	295	<i>Flad et al.</i> [2006]		Estimated
J_{5a}	$\text{HCHO} \rightarrow \text{HCO} + \text{H}$	225–375	223	<i>Meller and Moortgat</i> [2000]	225–250	<i>Glicker and Stief</i> [1971]
J_{5b}	$\rightarrow \text{CO} + \text{H}_2$				250–375	<i>Sander et al.</i> [2006]
J_{5c}	$\rightarrow \text{CO} + \text{H} + \text{H}$					

^aThis channel produces excited CO (CO*), which we assume is quickly deexcited to the ground state.

densities. The value of K in the upper atmosphere is best constrained by INMS measurements of the ^{40}Ar distribution [Yelle *et al.*, 2008]. In order to match both these constraints we adopt the following form for the eddy profile,

$$K(z) = \frac{K_o(p_o/p)^\gamma K_\infty}{K_o(p_o/p)^\gamma + K_\infty}, \quad (2)$$

where p is the pressure, $p_o = 1.77 \times 10^3$ Pa and $\gamma = 2.0$ [Yelle *et al.*, 2008]. Of primary importance here is the value

of K in the lower stratosphere which is controlled by the K_o parameter. We adopt $K_\infty = 3 \times 10^7 \text{ cm}^2 \text{ s}^{-1}$ for all models presented here but consider several values for K_o . Figure 2 shows a typical K profile with $K_o = 4 \times 10^2 \text{ cm}^2 \text{ s}^{-1}$.

[27] Molecular diffusion is also included in the model using molecular diffusion coefficients, D , primarily from Mason and Marrero [1970]. However, we were unable to find published measurements or models for the diffusion coefficient for HCHO in N_2 . In this case, we follow the prescription outlined by Hirschfelder *et al.* [1964] and use

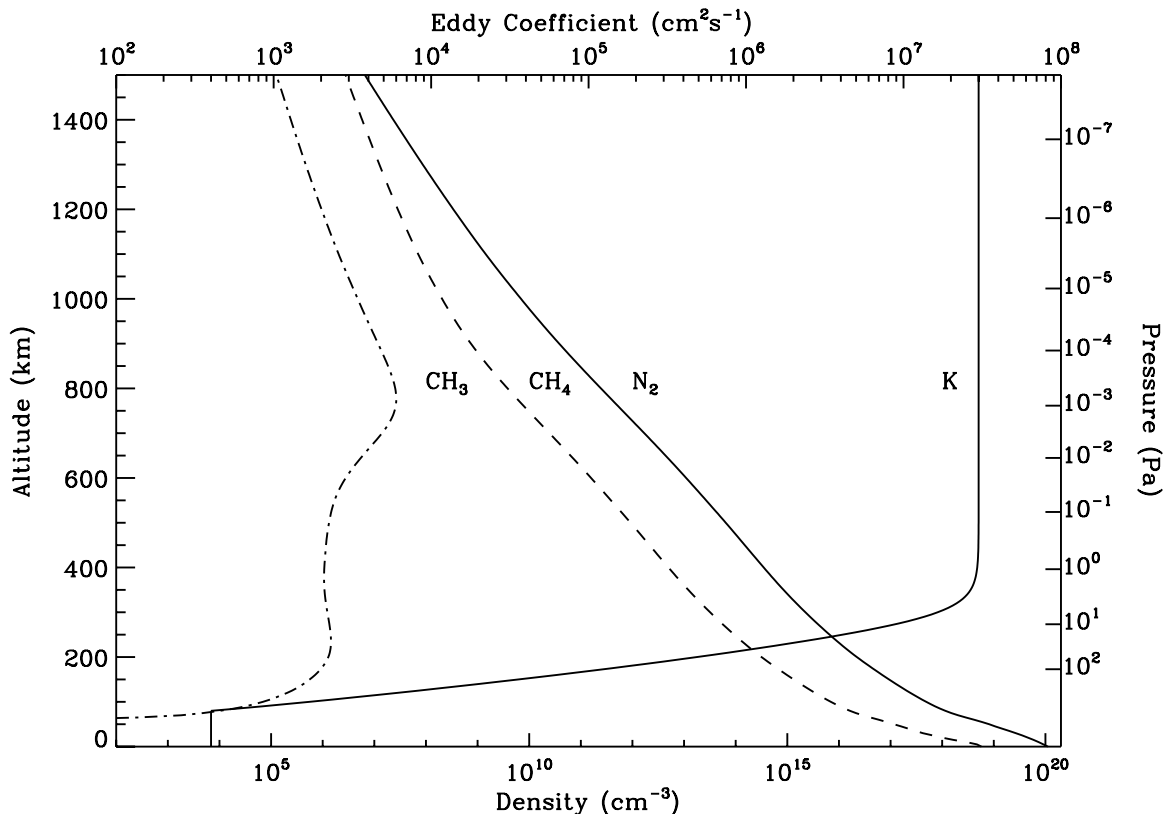


Figure 2. The densities of CH_3 , CH_4 , and N_2 as a function of altitude. Also plotted is the eddy diffusion profile adopted in this study.

the collision integrals based on the Lennard-Jones potential and force constants for N₂ and HCHO to estimate the diffusion coefficient of HCHO in N₂. With the temperature-pressure profile, eddy profile, and molecular diffusion coefficients we can calculate the N₂ and CH₄ distributions, as shown in Figure 2. The densities of these constituents are treated as fixed as N₂ and CH₄ are far too abundant to be altered by oxygen chemistry.

[28] The distribution of oxygen-bearing species is computed by solving the coupled continuity and diffusion equations. The continuity equation is

$$\frac{dN_i}{dt} = P_i - L_i - \frac{1}{r^2} \frac{\partial}{\partial r} r^2 \Phi_i, \quad (3)$$

where P_i and L_i represent chemical production and loss and the third term is the divergence of the diffusive flux, Φ_i . The flux is given by

$$\Phi_i = -D_i \left(\frac{\partial N_i}{dr} + \frac{N_i}{H_i} + \frac{(1 + \alpha) N_i}{T} \frac{\partial T}{\partial r} \right) - K \left(\frac{\partial N_i}{dr} + \frac{N_i}{H_a} + \frac{N_i}{T} \frac{\partial T}{\partial r} \right), \quad (4)$$

where H_i is the diffusive equilibrium scale height for the i th species, H_a is the scale height for the background atmosphere, and α is the thermal diffusion coefficient. Boundary conditions depend on the chemical species. Radicals are assumed to be in chemical equilibrium at the lower boundary. Noncondensing species have zero velocity at the lower boundary. H and H₂ escape from the upper boundary as described by *Yelle et al.* [2008]. All other species are assumed to be in diffusive equilibrium. CH₄ is not calculated in the model; it is held fixed with the profile presented by *Yelle et al.* [2008]. The equations are converted to difference equations on a finite grid with a spacing of 5 km and are solved by integrating to a steady state, at which time the 3 terms on the right-hand side of the continuity equation balance to better than 10⁻⁸ times the value of the largest term. Calculations are typically run for at least 10¹⁴ seconds resulting in a steady state for even the most inert species such as CO.

[29] Photodissociation processes and chemical reactions included in the model are listed in Tables 3 and 4 and are discussed further below. Photolysis rates are computed for a global average, estimated as half the rate at a solar zenith angle of 60 degrees [*Lebonnois and Toublanc*, 1999]. We represent the solar flux with the EUVAC proxy model [*Richards et al.*, 1994]. Sources for the photoabsorption cross sections and branching ratios are listed in Table 4. We adopt a total aerosol optical depth in the UV of 15 and assume that it is independent of wavelength. Better constraints on the FUV properties of the aerosols are needed, but the uncertainty caused by this assumption is less than other aspects of the model (e.g., O⁺ flux) and will not alter our conclusion. Rayleigh scattering is taken into account using the cross sections of *Dalgarno et al.* [1967]. The scattered radiation field is calculated using a two-stream approximation.

[30] The only sources of oxygen in our model are the precipitation of O⁺ ions from the magnetosphere into the

upper atmosphere and the inflow of OH or H₂O. We model these as distributed production rates in the upper atmosphere assuming a Chapman production function with a peak at 1100 km for O⁺ (from the O⁺ deposition calculations) and 750 km for OH or H₂O as calculated by *English et al.* [1996]. The details of the production function can affect densities at and above the deposition altitude somewhat, but for the lower atmosphere the only significant quantity is the column-integrated production rate, which determines the flux to the lower atmosphere. In particular, the densities in the lower atmosphere are not strongly dependent on the peak deposition altitude. The only loss in the model is condensation in the troposphere. The condensation rate is assumed proportional to the excess atmospheric pressure over the local vapor pressure with a constant of proportionality chosen to insure insignificant supersaturation. Under Titan conditions CO does not condense at all; therefore loss of oxygen occurs only through condensation of CO₂ and H₂O. At lower values of K_o the rate of CO₂ condensation greatly exceeds that of H₂O; at higher values of K_o the condensation rates of CO₂ and H₂O are approximately equal. Other oxygen-bearing species (HCHO, HCO, OH, etc.) have densities that are too small for condensation to occur in the atmosphere; these species condense directly on the surface, but their abundances are so small that this makes a negligible contribution to the overall balance.

4. Results and Discussion

[31] Since the stratospheric abundances of photochemically produced species are highly dependent on the value of the eddy coefficient in the lower atmosphere, we investigated six values ranging from $K_o = 1 \times 10^2 \text{ cm}^2 \text{ s}^{-1}$ to $K_o = 1 \times 10^3 \text{ cm}^2 \text{ s}^{-1}$. We adjusted the values of the input fluxes of O and OH to reproduce the observed abundances of CO and CO₂. The ability to reproduce the H₂O observations is an important test for the model. Table 5 lists input parameters and key output parameters for several model runs. We discuss model D in detail because the input fluxes of O and OH are closest to the nominal values of *Hartle et al.* [2006], *Feuchtgruber et al.* [1997], and *English et al.* [1996] and the value of $K_o = 4 \times 10^2 \text{ cm}^2 \text{ s}^{-1}$ used in model D has been shown to accurately reproduce CIRS observations of hydrocarbon species [*Vuitton et al.*, 2008] and is similar to the value derived from CIRS observations [*Vinatiev et al.*, 2007]. The mole fractions of the most abundant oxygen-bearing species for model D are shown in Figure 3, the primary photodissociation rates are shown in Figure 4, and the important chemical reaction rates are shown in Figure 5. Model D adequately matches all the observational constraints, including H₂O.

[32] Unlike all previous photochemical models, the main CO production pathway is the reaction of O with CH₃, which produces CO directly (k_{7b}) or indirectly through formation of HCHO in this same reaction (k_{7a}). The HCHO is photolyzed to produce CO (k_{5b} , k_{5c}) or HCO (k_{5a}). The HCO reacts with H or CH₃ to again produce CO (k_{17} , k_{18}). The important reaction rates are shown in Figure 5. The net result is that essentially all of the input O is converted quickly to CO. These processes occur primarily in the upper atmosphere.

Table 5. Model Runs^a

Model	K_o	Input ($\text{cm}^{-2} \text{s}^{-1}$)		Condensation ($\text{cm}^{-2} \text{s}^{-1}$)		Mole Fraction		
		$\text{O}(^3\text{P})$	OH	CO_2	H_2O	150 km		400 km
						CO	CO_2	H_2O
A	1.0×10^2	3.3×10^5	6.2×10^5	4.5×10^5	3.1×10^4	5.1×10^{-5}	1.5×10^{-8}	1.0×10^{-9}
B	2.0×10^2	7.7×10^5	1.2×10^6	9.0×10^5	1.5×10^5	5.1×10^{-5}	1.5×10^{-8}	1.7×10^{-9}
C	3.0×10^2	1.2×10^6	1.9×10^6	1.4×10^6	3.5×10^5	5.1×10^{-5}	1.5×10^{-8}	2.4×10^{-9}
D	4.0×10^2	1.6×10^6	2.6×10^6	1.8×10^6	6.5×10^5	5.1×10^{-5}	1.5×10^{-8}	3.1×10^{-9}
E	6.0×10^2	2.5×10^6	4.4×10^6	2.7×10^6	1.5×10^6	5.0×10^{-5}	1.5×10^{-8}	4.7×10^{-9}
F	1.0×10^3	4.2×10^6	9.0×10^6	4.5×10^6	4.3×10^6	5.0×10^{-5}	1.5×10^{-8}	7.9×10^{-9}

^aThe fluxes are referred to the surface.

The main production peak for CO occurs at ~ 1100 km, where $\text{O}(^3\text{P})$ is primarily deposited. A secondary peak at ~ 200 km arises following the production of O atoms and CO by CO_2 photolysis (J_3).

[33] The observed O^+ influx rate of $\sim 10^6 \text{ cm}^{-2} \text{ s}^{-1}$ [Hartle *et al.*, 2006] can supply the observed abundance of CO in Titan's atmosphere in approximately 300 Ma, much shorter than the age of the solar system. If O^+ has been incident upon Titan for longer than that, a loss process is needed to limit the buildup of CO in the atmosphere. Once formed, CO is difficult to remove. CO does not condense in Titan's atmosphere and direct CO photolysis is negligible because it is shielded by the far more abundant N_2 . The only loss is through reaction with OH (k_{16}), which

occurs from 100 to 600 km with a maximum rate of $0.1 \text{ cm}^{-3} \text{ s}^{-1}$ in model D. The net loss rate of CO is equal to loss through CO_2 formation minus the production from CO_2 photolysis. The column-integrated rates for these processes are $1.91 \times 10^6 \text{ cm}^{-2} \text{ s}^{-1}$ and $1.22 \times 10^5 \text{ cm}^{-2} \text{ s}^{-1}$. Neglecting smaller channels involving HCHO, the difference is equal to the sum of the input O flux and the oxygen produced by CO_2 photolysis. Since CO is inert and has essentially the same molecular weight as N_2 , it is efficiently redistributed by diffusion resulting in a calculated mole fraction that is constant throughout the atmosphere at 5×10^{-5} .

[34] CO_2 is produced through reaction of CO and OH. The CO_2 mole fraction decreases at high altitudes due to

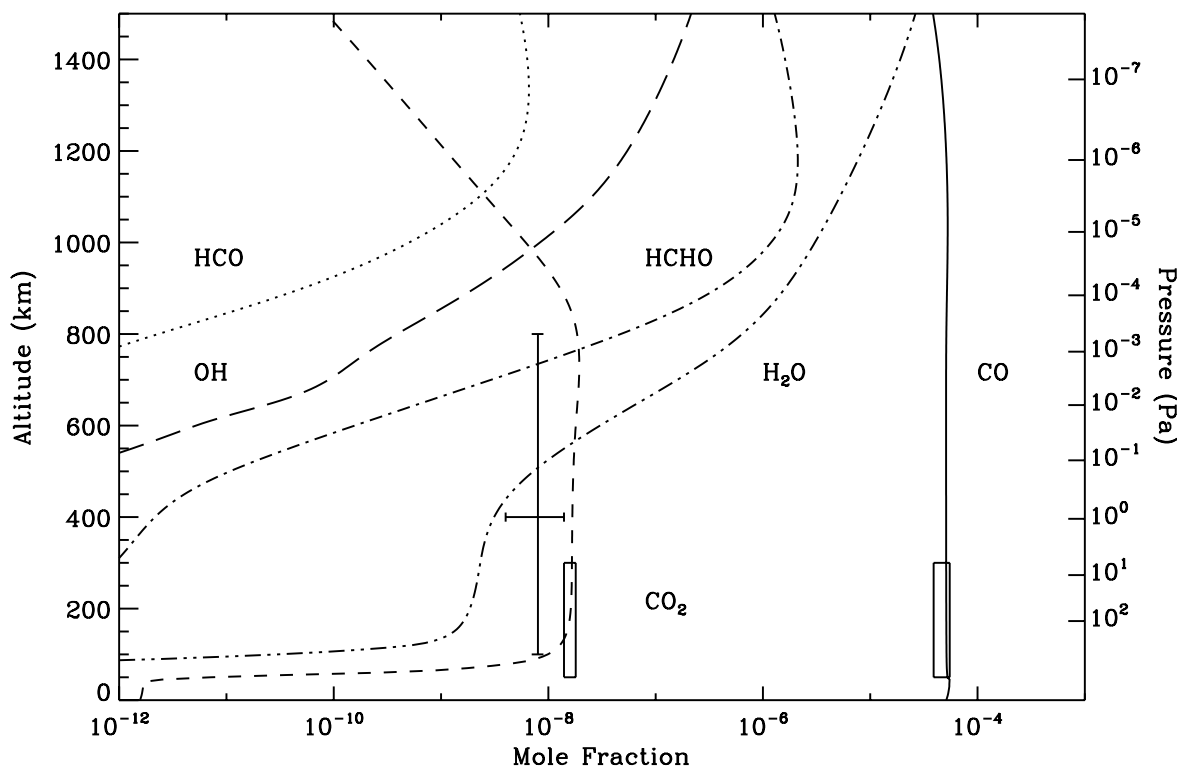


Figure 3. The mole fraction of CO_2 (dashed), H_2O (dash-double dotted), CO (solid), HCHO (dash-dotted), HCO (dotted), and OH (long dashed) as a function of altitude for $K_o = 4. \times 10^{-2} \text{ cm}^2 \text{ s}^{-1}$ from model D. The horizontal bar represents the derived mole fraction of H_2O , and the vertical line indicates the width of the contribution function from the ISO observations [Coustonis *et al.*, 1998]. The boxes represent CIRS observations of CO and CO_2 [de Kok *et al.*, 2007]. The mole fractions are inferred to be constant with altitude within the boxes.

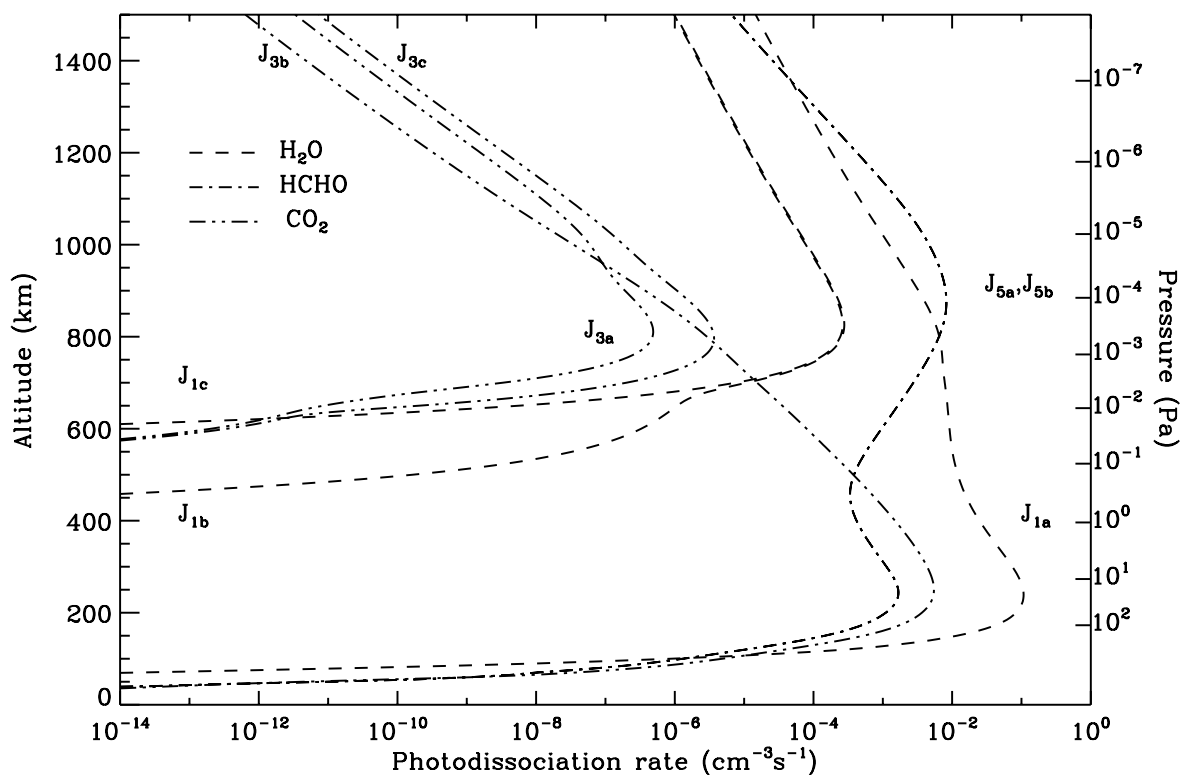


Figure 4. Photodissociation rates for the major oxygen species. The dashed lines are H₂O, the dash-dotted lines are HCHO, and the dash-double dotted lines are CO₂. The products are described in Table 4.

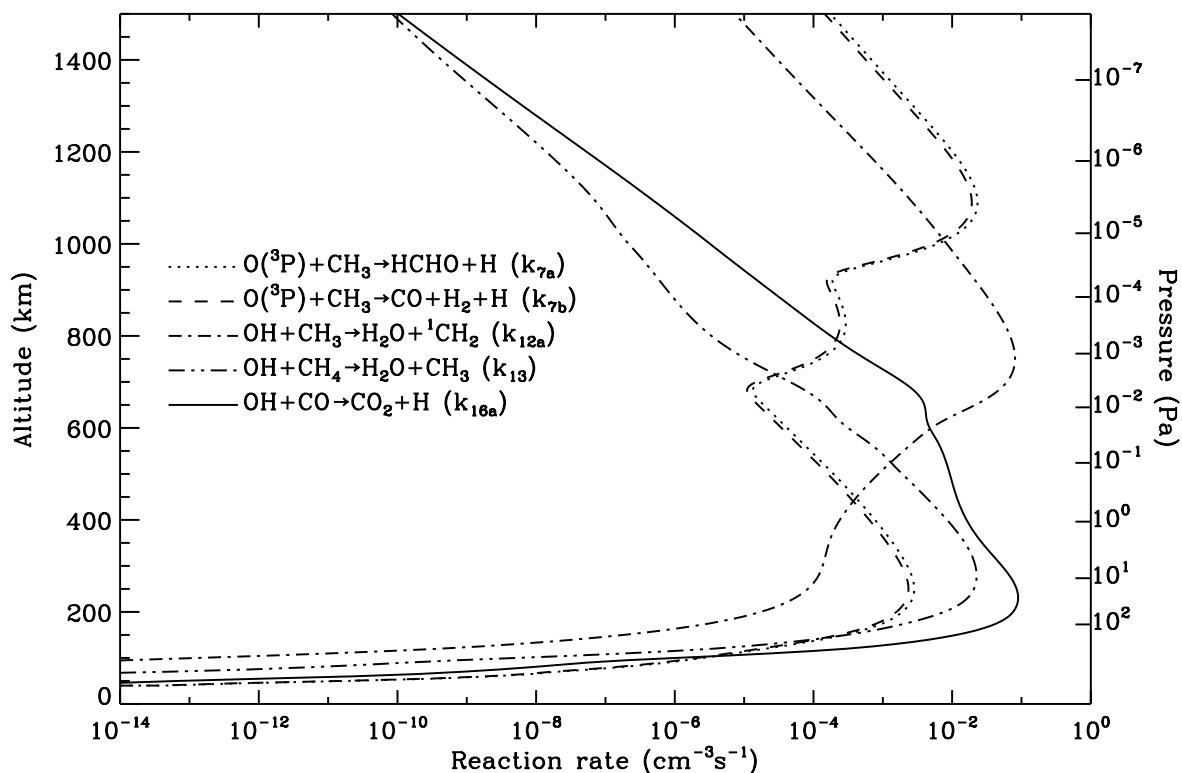


Figure 5. Important reaction rates as a function of altitude. The dotted line is O(³P) + CH₃ → HCHO + H, the dashed line is O(³P) + CH₃ → CO + H₂ + H, the dash-dotted line is OH + CH₃ → H₂O + ¹CH₂, the dash-double dotted line is OH + CH₄ → H₂O + CH₃, and the solid line is OH + CO → CO₂ + H.

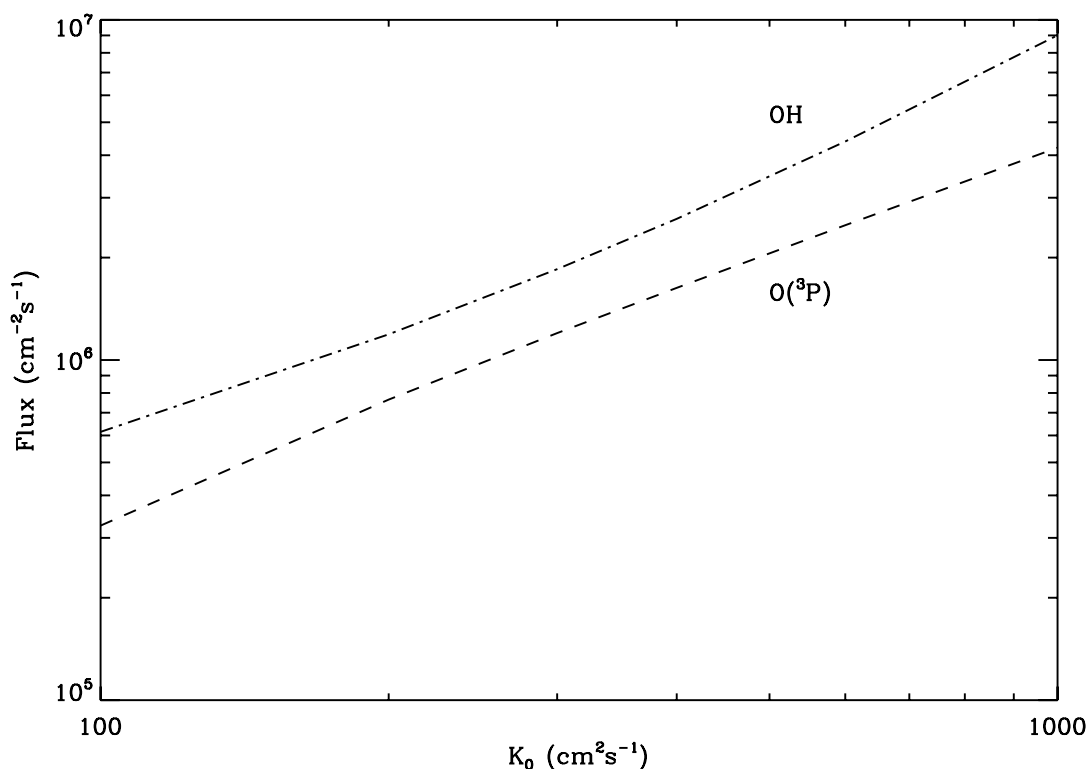


Figure 6. OH and O(³P) fluxes required to reproduce a CO mole fraction of 5×10^{-5} and CO₂ mole fraction of 1.5×10^{-8} at 150 km as a function of eddy diffusion coefficient in Titan's lower atmosphere (K_0).

diffusive separation but is relatively constant in the stratosphere with a value of 1.5×10^{-8} . The mole fraction decreases toward the lower atmosphere as CO₂ diffuses downward into the condensation region. CO₂ production peaks at ~ 200 km altitude (k_{16}) and peak CO₂ photodissociation occurs at 250 km with a rate of $5.5 \times 10^{-3} \text{ cm}^{-3} \text{ s}^{-1}$. Loss is due to photolysis and condensation. The column-integrated condensation rate for model D is $1.79 \times 10^6 \text{ cm}^{-2} \text{ s}^{-1}$, while the column-integrated photolysis rate is $1.22 \times 10^{-5} \text{ cm}^{-2} \text{ s}^{-1}$; condensation is responsible for approximately two thirds of the CO₂ loss for this model. As shown in Table 5, twice the column-integrated condensation rate of CO₂ is precisely the sum of O and OH fluxes minus the column-integrated condensation rate of H₂O. The CO₂ condensation rates for our models correspond to the accumulation of tens of centimeters to a meter of CO₂ on the surface over the age of the solar system. *McCord et al.* [2008] modeled VIMS spectra using CO₂ frost on the surface, but our condensation rate is 3 orders of magnitude less than that of C₂H₆ so it is unclear if the smaller amount of CO₂ would be detectable.

[35] As previously discussed, any OH in Titan's upper atmosphere is immediately converted to H₂O through reactions with CH₃. However, there is a small steady state abundance of OH due to photolysis of H₂O. It is this OH population that is responsible for destroying CO and forming CO₂. For model D, photolysis is the dominant H₂O loss mechanism with a column-integrated value of $2.83 \times 10^6 \text{ cm}^{-2} \text{ s}^{-1}$. Condensation plays an increasingly important role as K_0 increases, and at $K_0 = 1 \times 10^3 \text{ cm}^2 \text{ s}^{-1}$ (model F) condensation is responsible for more than half

the H₂O loss. The calculated H₂O mole fraction increases with increasing altitude and has a value 3.1×10^{-9} at 400 km, consistent with the observed abundance of H₂O of $8^{+6}_{-4} \times 10^{-9}$ [Coustonis et al., 1998].

[36] These general characteristics of all the models listed in Table 5 are the same, but some of the details do differ. Figure 6 shows the dependence of the O and OH fluxes required to match the observed CO and CO₂ mole fractions as a function of K_0 . In general, the ratio of the OH and O fluxes controls the CO₂ abundance and the magnitude of these fluxes determines the CO mole fraction. In most cases, the OH flux required to produce the observed CO₂ abundance is a little less than twice the O flux. Larger values of K_0 require larger fluxes because the molecules formed in the upper atmosphere are transported to the loss region in the lower atmosphere more quickly. It is a strong argument in favor of this model that calculations with the accepted values of K_0 and the input O flux consistent with the magnetospheric measurements predicted mole fractions for oxygen-bearing species in agreement with observational constraints.

5. Summary

[37] We demonstrate that the observed densities of CO, CO₂, and H₂O can be explained by a combination of O and OH or H₂O input to the upper atmosphere. It is essential to have sources of both atomic oxygen and OH or H₂O in order to produce both CO and CO₂. Input of O alone produces only CO, and with only O input there is no effective loss process for CO and steady state solutions

are not possible. Input of OH or H₂O alone does not produce CO and only produces CO₂ if CO is already present.

[38] Production of both CO and CO₂ by only H₂O influx, considered in several previous investigations [Yung *et al.*, 1984; Toublanc *et al.*, 1995; Lara *et al.*, 1996] and adopted as an explanation in several observational papers, is not possible. The previous studies that employed this assumption were able to match observations only because incorrect products were assumed for the reaction of OH and CH₃. The investigations by Wong *et al.* [2002] and Wilson and Atreya [2004] employed the correct chemistry, but were still unable to reproduce the observed CO abundances. They attempted to explain the observations by invoking an internal source of CO in addition to an external source of H₂O or by assuming that the observed CO is the remnant of a larger primordial abundance. We show that, given the detection of O⁺ precipitating into Titan's upper atmosphere, it is no longer necessary to invoke outgassing from Titan's interior as a source for atmospheric CO or to assume that the observed CO is the remnant of a larger primordial abundance in Titan's atmosphere. Instead, it is most likely that the oxygen bearing species in Titan's atmosphere are the result of external input. The flux of O⁺ into Titan's atmosphere represents only 10⁻⁴ of the estimated H₂O source rate at Enceladus [Hartle *et al.*, 2006; Hansen *et al.*, 2006], suggesting that the possibility of an Enceladus source deserves further investigation. This small flux nevertheless is responsible for synthesis of CO, the fourth most abundant molecule in Titan's atmosphere.

[39] **Acknowledgment.** We acknowledge support from NASA grant NNG05G085G.

References

- Adachi, H., N. Basco, and D. James (1981), The acetyl radicals CH₃CO and CD₃CO studied by flash-photolysis and kinetic spectroscopy, *Int. J. Chem. Kinetics*, *13*(12), 1251–1276.
- Atkinson, R., D. L. Baulch, R. A. Cox, J. N. Crowley, R. F. Hampson, R. G. Hynes, M. E. Jenkin, M. J. Rossi, and J. Troe (2004), Evaluated kinetic and photochemical data for atmospheric chemistry: Volume I – Gas phase reactions of O_x, HO_x, NO_x and SO_x species, *Atmos. Chem. Phys.*, *4*, 1461–1738.
- Atkinson, R., D. L. Baulch, R. A. Cox, J. N. Crowley, R. F. Hampson, R. G. Hynes, M. E. Jenkin, M. J. Rossi, and J. Troe (2006), Evaluated kinetic and photochemical data for atmospheric chemistry: Volume II – Gas phase reactions of organic species, *Atmos. Chem. Phys.*, *6*, 3625–4055.
- Atreya, S. K., T. M. Donahue, and W. R. Kuhn (1978), Evolution of a nitrogen atmosphere on Titan, *Science*, *201*, 611–613.
- Atreya, S. K., E. Y. Adams, H. B. Niemann, J. E. Demick-Montelara, T. C. Owen, M. Fulchignoni, F. Ferri, and E. H. Wilson (2006), Titan's methane cycle, *Planet. Space Sci.*, *54*, 1177–1187, doi:10.1016/j.pss.2006.05.028.
- Baines, K. H., P. Drossart, M. A. Lopez-Valverde, S. K. Atreya, C. Sotin, T. W. Momary, R. H. Brown, B. J. Buratti, R. N. Clark, and P. D. Nicholson (2006), On the discovery of CO nighttime emissions on Titan by Cassini/VIMS: Derived stratospheric abundances and geological implications, *Planet. Space Sci.*, *54*, 1552–1562, doi:10.1016/j.pss.2006.06.020.
- Baulch, D. L., *et al.* (1992), Evaluated kinetic data for combustion modeling, *J. Phys. Chem. Ref. Data*, *21*, 411–734.
- Baulch, D. L., *et al.* (1994), Evaluated kinetic data for combustion modeling. Supplement I, *J. Phys. Chem. Ref. Data*, *23*, 847–848.
- Chan, W., G. Cooper, and C. Brion (1993a), The electronic-spectrum of water in the discrete and continuum regions- absolute optical oscillator-strengths for photoabsorption (6–200 eV), *Chem. Phys.*, *178*(1–3), 387–400.
- Chan, W., G. Cooper, and C. Brion (1993b), Absolute optical oscillator-strengths for discrete and continuum photoabsorption of carbon-monoxide (7–200 eV) and transition moments for the X¹Σ⁺ → A¹Π system, *Chem. Phys.*, *170*(1), 123–138.
- Chan, W., G. Cooper, and C. Brion (1993c), The electronic-spectrum of carbon-dioxide- discrete and continuum photoabsorption oscillator-strengths (6–203 eV), *Chem. Phys.*, *178*(1–3), 401–413.
- Cook, G. R., P. H. Metzger, and M. Ogawa (1965), Photoionization and absorption coefficients of CO in the 600 to 1000 Å region, *Canadian Journal of Physics*, *43*, 1706.
- Coustonis, A., and B. Bezdard (1995), Titan's atmosphere from Voyager infrared observations. IV – Latitudinal variations of temperature and composition, *Icarus*, *115*, 126–140, doi:10.1006/icar.1995.1084.
- Coustonis, A., B. Bezdard, and D. Gautier (1989), Titan's atmosphere from Voyager infrared observations. I – The gas composition of Titan's equatorial region, *Icarus*, *80*, 54–76, doi:10.1016/0019-1035(89)90161-9.
- Coustonis, A., B. Bezdard, D. Gautier, A. Marten, and R. Samuelson (1991), Titan's atmosphere from Voyager infrared observations. III – Vertical contributions of hydrocarbons and nitriles near Titan's north pole, *Icarus*, *89*, 152–167, doi:10.1016/0019-1035(91)90095-B.
- Coustonis, A., A. Salama, E. Lellouch, T. Encrenaz, G. L. Bjoraker, R. E. Samuelson, T. de Graauw, H. Feuchtgruber, and M. F. Kessler (1998), Evidence for water vapor in Titan's atmosphere from ISO/SWS data, *Astron. Astrophys.*, *336*, L85–L89.
- Coustonis, A., A. Salama, B. Schulz, S. Ott, E. Lellouch, T. H. Encrenaz, D. Gautier, and H. Feuchtgruber (2003), Titan's atmosphere from ISO mid-infrared spectroscopy, *Icarus*, *161*, 383–403, doi:10.1016/S0019-1035(02)00028-3.
- Coustonis, A., *et al.* (2007), The composition of Titan's stratosphere from Cassini/CIRS mid-infrared spectra, *Icarus*, *189*, 35–62, doi:10.1016/j.icarus.2006.12.022.
- Dalgarno, A., T. Degges, and D. A. Williams (1967), Dipole properties of molecular nitrogen, *Proc. Phys. Soc. London*, *92*, 291–295.
- Davidson, J. A., H. I. Schiff, T. J. Brown, and C. J. Howard (1978), Temperature dependence of the deactivation of O¹D by CO from 113–333 K, *J. Chem. Phys.*, *69*, 1216–+.
- de Kok, R., *et al.* (2007), Oxygen compounds in Titan's stratosphere as observed by Cassini CIRS, *Icarus*, *186*, 354–363, doi:10.1016/j.icarus.2006.09.016.
- Dougherty, M. K., K. K. Khurana, F. M. Neubauer, C. T. Russell, J. Saur, J. S. Leisner, and M. E. Burton (2006), Identification of a dynamic atmosphere at Enceladus with the Cassini magnetometer, *Science*, *311*, 1406–1409, doi:10.1126/science.1120985.
- Dubouloz, N., F. Raulin, E. Lellouch, and D. Gautier (1989), Titan's hypothesized ocean properties—The influence of surface temperature and atmospheric composition uncertainties, *Icarus*, *82*, 81–96, doi:10.1016/0019-1035(89)90025-0.
- Edgar, B. C., H. S. Porter, and A. E. S. Green (1975), Proton energy deposition in molecular and atomic oxygen and applications to the polar cap, *Planet. Space Sci.*, *23*, 787–804, doi:10.1016/0032-0633(75)90015-X.
- English, M. A., L. M. Lara, R. D. Lorenz, P. R. Ratcliff, and R. Rodrigo (1996), Ablation and chemistry of meteoric materials in the atmosphere of Titan, *Adv. Space Res.*, *17*, 157–160.
- Esposito, L. W., *et al.* (2005), Ultraviolet imaging spectroscopy shows an active saturnian system, *Science*, *307*, 1251–1255, doi:10.1126/science.1105606.
- Feuchtgruber, H., E. Lellouch, T. de Graauw, B. Bezdard, T. Encrenaz, and M. Griffin (1997), External supply of oxygen to the atmospheres of giant planets, *Nature*, *389*, 159–162.
- Flad, J., S. Brown, J. Burkholder, H. Stark, and A. Ravishankara (2006), Absorption cross sections for the A²A¹ (0,0,0) ← X²A¹ (0,0,0) band of the HCO radical, *Phys. Chem. Chem. Phys.*, *8*(31), 3636–3642.
- Flasar, F. M., *et al.* (2005), Titan's atmospheric temperatures, winds, and composition, *Science*, *308*, 975–978, doi:10.1126/science.1111150.
- Fulchignoni, M., *et al.* (2005), In situ measurements of the physical characteristics of Titan's environment, *Nature*, *438*, 785–791, doi:10.1038/nature04314.
- Glicker, S., and L. Stief (1971), Photolysis of formaldehyde at 1470 and 1236 Å, *J. Chem. Phys.*, *54*(7), 2852.
- Gurwell, M. A. (2004), Submillimeter observations of Titan: Global measures of stratospheric temperature, CO, HCN, HC₃N, and the isotopic ratios ¹²C/¹³C and ¹⁴N/¹⁵N, *Astrophys J.*, *616*, L7–L10, doi:10.1086/423954.
- Gurwell, M. A., and D. O. Muhleman (1995), CO on Titan: evidence for a well-mixed vertical profile, *Icarus*, *117*, 375–382, doi:10.1006/icar.1995.1163.
- Gurwell, M. A., and D. O. Muhleman (2000), Note: CO on Titan: More evidence for a well-mixed vertical profile, *Icarus*, *145*, 653–656, doi:10.1006/icar.2000.6424.
- Hack, W., M. Hold, K. Hoyerermann, J. Wehmeyer, and T. Zeuch (2005), Mechanism and rate of the reaction CH₃ + O⁻ revisited, *Phys. Chem. Chem. Phys.*, *7*(9), 1977–1984.

- Hansen, C. J., L. Esposito, A. I. F. Stewart, J. Colwell, A. Hendrix, W. Pryor, D. Shemansky, and R. West (2006), Enceladus' water vapor plume, *Science*, *311*, 1422–1425, doi:10.1126/science.1121254.
- Harich, S., J. J. Lin, Y. T. Lee, and X. Yang (1999), Competing atomic and molecular hydrogen pathways in the photodissociation of methanol at 157 nm, *J. Chem. Phys.*, *111*, 5–9, doi:10.1063/1.479249.
- Hartle, R. E., et al. (2006), Preliminary interpretation of Titan plasma interaction as observed by the Cassini Plasma Spectrometer: Comparisons with Voyager 1, *Geophys. Res. Lett.*, *33*, L08201, doi:10.1029/2005GL024817.
- Hassinen, E., K. Kalliorinne, and J. Koskikallio (1990), Kinetics of reactions between methyl and acetyl radicals in gas-phase produced by flash-photolysis of acetic-anhydride, *Int. J. Chem. Kinetics*, *22*(7), 741–745.
- Hidayat, T., A. Marten, B. Bezaud, D. Gautier, T. Owen, H. E. Matthews, and G. Paubert (1998), Millimeter and submillimeter heterodyne observations of Titan: The vertical profile of carbon monoxide in its stratosphere, *Icarus*, *133*, 109–133, doi:10.1006/icar.1998.5908.
- Hirschfelder, J. O., C. F. Curtiss, and R. B. Bird (1964), *Molecular Theory of Gases and Liquids*, John Wiley, New York.
- Horányi, M., A. Juhász, and G. E. Morfill (2008), Large-scale structure of Saturn's E-ring, *Geophys. Res. Lett.*, *35*, L04203, doi:10.1029/2007GL032726.
- Ishimoto, M., G. J. Romick, and C.-I. Meng (1992), Energy distribution of energetic O(+) precipitation into the atmosphere, *J. Geophys. Res.*, *97*, 8619–8629.
- Johnson, R. E. (1990), *Energetic Charged-Particle Interactions With Atmospheres and Surfaces*, Springer, Berlin.
- Koyano, I., T. S. Wauchop, and K. H. Welge (1975), Relative efficiencies of O(¹S) production from photodissociation of CO₂ between 1080 and 1160 Å, *J. Chem. Phys.*, *63*, 110–113.
- Lara, L. M., E. Lellouch, J. J. López-Moreno, and R. Rodrigo (1996), Vertical distribution of Titan's atmospheric neutral constituents, *J. Geophys. Res.*, *101*, 23,261–23,283, doi:10.1029/96JE02036.
- Lawrence, G. (1972), Production of O(¹S) from photodissociation of CO₂, *J. Chem. Phys.*, *57*(12), 5616.
- Lebonnois, S., and D. Toublanc (1999), Actinic fluxes in Titan's atmosphere, from one to three dimensions: Application to high-latitude composition, *J. Geophys. Res.*, *104*, 22,025–22,034, doi:10.1029/1999JE001056.
- Lellouch, E., A. Coustenis, B. Sebag, J.-G. Cuby, M. López-Valverde, B. Schmitt, T. Fouchet, and J. Crovisier (2003), Titan's 5- μ m window: Observations with the very large telescope, *Icarus*, *162*, 125–142, doi:10.1016/S0019-1035(02)00079-9.
- Letourneur, B., and A. Coustenis (1993), Titan's atmospheric structure from Voyager 2 infrared spectra, *Planet. Space Sci.*, *41*, 593–602, doi:10.1016/0032-0633(93)90079-H.
- Lindsay, B. G., R. L. Merrill, H. C. Straub, K. A. Smith, and R. F. Stebbings (1998), Absolute differential and integral cross sections for charge transfer of keV O⁺ with N₂, *Phys. Rev. A*, *57*, 331–337, doi:10.1103/PhysRevA.57.331.
- López-Valverde, M. A., E. Lellouch, and A. Coustenis (2005), Carbon monoxide fluorescence from Titan's atmosphere, *Icarus*, *175*, 503–521, doi:10.1016/j.icarus.2004.12.015.
- Lutz, B. L., C. de Bergh, and T. Owen (1983), Titan—Discovery of carbon monoxide in its atmosphere, *Science*, *220*, 1374–+.
- Marten, A., D. Gautier, L. Tanguy, A. Lecacheux, and C. Rosolen (1988), Abundance of carbon monoxide in the stratosphere of Titan from millimeter heterodyne observations, *Icarus*, *76*, 558–562, doi:10.1016/0019-1035(88)90021-8.
- Mason, E. A., and T. R. Marrero (1970), The diffusion of atoms and molecules, *Adv. At. Mol. Phys.*, *6*, 155–232.
- McCord, T. B., et al. (2008), Titan's surface: Search for spectral diversity and composition using the Cassini VIMS investigation, *Icarus*, *194*, 212–242, doi:10.1016/j.icarus.2007.08.039.
- McKay, C. P., T. W. Scattergood, J. B. Pollack, W. J. Borucki, and H. T. van Ghysseghem (1988), High-temperature shock formation of N₂ and organics on primordial Titan, *Nature*, *332*, 520–522, doi:10.1038/332520a0.
- Meller, R., and G. K. Moortgat (2000), Temperature dependence of the absorption cross sections of formaldehyde between 223 and 323 K in the wavelength range 225–375 nm, *J. Geophys. Res.*, *105*, 7089–7102, doi:10.1029/1999JD901074.
- Moran, T. F., and J. B. Wilcox (1978), Charge transfer reactions of ground O⁺(⁴S) and excited O⁺(²D) state ions with neutral molecules, *J. Chem. Phys.*, *69*, 1397–1405.
- Mordaunt, D. H., M. N. R. Ashfold, and R. N. Dixon (1994), Dissociation dynamics of H₂O(D₂O) following photoexcitation at the Lyman- α wavelength (121.6 nm), *J. Chem. Phys.*, *100*, 7360–7375.
- Mota, R., et al. (2005), Water VUV electronic state spectroscopy by synchrotron radiation, *Chem. Phys. Lett.*, *416*, 152–159.
- Mousis, O., D. Gautier, and D. Bockelée-Morvan (2002), An Evolutionary Turbulent Model of Saturn's Subnebula: Implications for the Origin of the Atmosphere of Titan, *Icarus*, *156*, 162–175, doi:10.1006/icar.2001.6782.
- Muhleman, D. O., G. L. Berge, and R. T. Clancy (1984), Microwave measurements of carbon monoxide on Titan, *Science*, *223*, 393–396.
- Müller-Wodarg, I. C. F., R. V. Yelle, J. Cui, and J. H. Waite (2008), Horizontal structures and dynamics of Titan's thermosphere, *J. Geophys. Res.*, *113*, E10005, doi:10.1029/2007JE003033.
- Niemann, H. B., et al. (2005), The abundances of constituents of Titan's atmosphere from the GCMS instrument on the Huygens probe, *Nature*, *438*, 779–784, doi:10.1038/nature04122.
- Noll, K. S., T. R. Geballe, R. F. Knacke, and Y. J. Pendleton (1996), Titan's 5 μ m spectral window: Carbon monoxide and the albedo of the surface, *Icarus*, *124*, 625–631, doi:10.1006/icar.1996.0236.
- Okabe, H. (1978), *Photochemistry of Small Molecules*, John Wiley, New York.
- Oser, H., N. D. Stothard, R. Humpfer, and H. H. Grotheer (1992), Direct measurement of the reaction CH₃ + OH at ambient temperature in the pressure range 0.3–6.2 mbar, *J. Phys. Chem.*, *96*, 5359–5363.
- Owen, T. (1982), The composition and origin of Titan's atmosphere, *Planet. Space Sci.*, *30*, 833–838, doi:10.1016/0032-0633(82)90115-5.
- Parkinson, W., J. Rufus, and K. Yoshino (2003), Absolute absorption cross section measurements of CO₂ in the wavelength region 163–200 nm and the temperature dependence, *Chem. Phys.*, *290*(2–3), 251–256.
- Pereira, R. A., D. L. Baulch, M. J. Pilling, S. H. Robertson, and G. Zeng (1997), Temperature and pressure dependence of the multichannel rate coefficients for the CH₃ + OH system, *J. Phys. Chem. A*, *101*, 9681–9693.
- Prinn, R. G., and B. Fegley Jr. (1981), Kinetic inhibition of CO and N₂ reduction in circumplanetary nebulae - Implications for satellite composition, *Astrophys. J.*, *249*, 308–317, doi:10.1086/159289.
- Richards, P. G., J. A. Fennelly, and D. G. Torr (1994), EUVAC: A solar EUV flux model for aeronomic calculations, *J. Geophys. Res.*, *99*, 8981–8992, (Correction to "EUVAC: A Solar EUV Flux Model for Aeronomic Calculations," *J. Geophys. Res.*, *99*, 13,283, 1994.)
- Samuelson, R. E., W. C. Maguire, R. A. Hanel, V. G. Kunde, D. E. Jennings, Y. L. Yung, and A. C. Aikin (1983), CO₂ on Titan, *J. Geophys. Res.*, *88*, 8709–8715.
- Samuelson, R. E., G. L. Bjoraker, A. Coustenis, E. Lellouch, A. Salama, and D. P. Hamilton (1998), Water influx at Titan, *Bull. Am. Astron. Soc.*, *30*, 1087.
- Sander, S. P., et al. (2006), Chemical kinetics and photochemical data for use in atmospheric studies, Evaluation Number 15, *JPL Publ.*, 06-02.
- Satyapal, S., J. Park, R. Bersohn, and B. Katz (1989), Dissociation of methanol and ethanol activated by a chemical reaction or by light, *J. Chem. Phys.*, *91*, 6873–6879.
- Shemansky, D. E. (1972), CO₂ extinction coefficient 1700–3000 Å, *J. Chem. Phys.*, *56*(4), 1582.
- Stief, L. J., W. A. Payne, and R. B. Klemm (1975), A flash photolysis-resonance fluorescence study of the formation of O(¹D) in the photolysis of water and the reaction of O(¹D) with H₂, Ar, and He, *J. Chem. Phys.*, *62*, 4000–4008.
- Toublanc, D., J. P. Parisot, J. Brillet, D. Gautier, F. Raulin, and C. P. McKay (1995), Photochemical modeling of Titan's atmosphere, *Icarus*, *113*, 2–26, doi:10.1006/icar.1995.1002.
- Tsang, W., and R. F. Hampson (1986), Chemical kinetic data base for combustion chemistry. Part I. Methane and related compounds, *J. Phys. Chem. Ref. Data*, *15*, 1087–1279.
- Tully, J. C. (1975), Reactions of O(¹D) with atmospheric molecules, *J. Chem. Phys.*, *62*, 1893–1898.
- Vanlook, H., and J. Peeters (1995), Rate coefficients of the reactions of C₂H with O₂, C₂H₂, and H₂O between 295 and 450 K, *J. Phys. Chem.*, *99*(44), 16,284–16,289.
- Vinater, S., et al. (2007), Vertical abundance profiles of hydrocarbons in Titan's atmosphere at 15°S and 80°N retrieved from Cassini/CIRS spectra, *Icarus*, *188*, 120–138, doi:10.1016/j.icarus.2006.10.031.
- Vuitton, V., J.-F. Doussin, Y. Bénéilan, F. Raulin, and M.-C. Gazeau (2006), Experimental and theoretical study of hydrocarbon photochemistry applied to Titan stratosphere, *Icarus*, *185*, 287–300, doi:10.1016/j.icarus.2006.06.002.
- Vuitton, V., R. V. Yelle, and M. J. McEwan (2007), Ion chemistry and N-containing molecules in Titan's upper atmosphere, *Icarus*, *191*, 722–742, doi:10.1016/j.icarus.2007.06.023.
- Vuitton, V., R. V. Yelle, and J. Cui (2008), Formation and distribution of benzene on Titan, *J. Geophys. Res.*, *113*, E05007, doi:10.1029/2007JE002997.
- Waite, J. H., et al. (2005a), Oxygen ions observed near Saturn's A ring, *Science*, *307*, 1260–1262, doi:10.1126/science.1105734.

- Waite, J. H., et al. (2005b), Ion Neutral Mass Spectrometer results from the first flyby of Titan, *Science*, *308*, 982–986, doi:10.1126/science.1110652.
- Waite, J. H., et al. (2006), Cassini Ion and Neutral Mass Spectrometer: Enceladus plume composition and structure, *Science*, *311*, 1419–1422, doi:10.1126/science.1121290.
- Wilson, E. H., and S. K. Atreya (2004), Current state of modeling the photochemistry of Titan's mutually dependent atmosphere and ionosphere, *J. Geophys. Res.*, *109*, E06002, doi:10.1029/2003JE002181.
- Wong, A.-S., C. G. Morgan, Y. L. Yung, and T. Owen (2002), Evolution of CO on Titan, *Icarus*, *155*, 382–392, doi:10.1006/icar.2001.6720.
- Yelle, R. V., J. Cui, and I. C. F. Müller-Wodarg (2008), Methane escape from Titan's atmosphere, *J. Geophys. Res.*, *113*, E10003, doi:10.1029/2007JE003031.
- Yoshino, K., J. R. Esmond, Y. Sun, W. H. Parkinson, K. Ito, and T. Matsui (1996), Absorption cross section measurements of carbon dioxide in the wavelength region 118.7 nm–175.5 nm and the temperature dependence, *J. Quant. Spectrosc. Radiat. Transfer*, *50*, 53–60.
- Yung, Y. L., M. Allen, and J. P. Pinto (1984), Photochemistry of the atmosphere of Titan—Comparison between model and observations, *Astrophys. J.*, *55*, 465–506, doi:10.1086/190963.
- Ziegler, J. F. (1980), *Handbook of Stopping Cross-Sections for Energetic Ions in All Elements*, Pergamon, New York.
- Ziegler, J. F. (1984), *Ion Implantation Science and Technology*, Academic, Orlando, Fla.
-
- S. M. Hörst and R. V. Yelle, Lunar and Planetary Laboratory, University of Arizona, 1629 E. University Boulevard, Tucson, AZ 85721, USA. (horst@lpl.arizona.edu; yelle@lpl.arizona.edu)
- V. Vuitton, Laboratoire de Planétologie de Grenoble, CNRS, Université Joseph Fourier, F-38041 Grenoble CEDEX 9, France. (veronique.vuitton@obs.ujf-grenoble.fr)